

# A fast doubly hybrid density functional method close to chemical accuracy using a local opposite spin ansatz

Igor Ying Zhang<sup>a,b</sup>, Xin Xu<sup>a,b,1</sup>, Yousung Jung<sup>c,1</sup>, and William A. Goddard III<sup>c,d,1</sup>

<sup>a</sup>Department of Chemistry, Shanghai Key Laboratory of Molecular Catalysis and Innovative Materials, Ministry of education (MOE) Laboratory for Computational Physical Science, Fudan University, Shanghai 200433, China; <sup>b</sup>State Key Laboratory of Physical Chemistry of Solid Surfaces, College for Chemistry and Chemical Engineering, Xiamen University, Xiamen 361005, China; <sup>c</sup>World Class University (WCU) Professor Program at the Graduate School of Energy, Environment, Water, and Sustainability (EEWS), Korea Advanced Institute of Science and Technology, Daejeon 305 701, Republic of Korea; and <sup>d</sup>Materials and Process Simulation Center (139 74), California Institute of Technology, Pasadena, CA 91125

Contributed by William A. Goddard III, September 21, 2011 (sent for review April 15, 2011)

**We develop and validate the XYGJ-OS functional, based on the adiabatic connection formalism and Görling-Levy perturbation theory to second order and using the opposite-spin (OS) ansatz combined with locality of electron correlation. XYGJ-OS with local implementation scales as  $N^3$  with an overall accuracy of 1.28 kcal/mol for thermochemistry, bond dissociation energies, reaction barrier heights, and nonbonded interactions, comparable to that of 1.06 kcal/mol for the accurate coupled-cluster based G3 method (scales as  $N^7$ ) and much better than many popular density functional theory methods: B3LYP (4.98), PBE0 (4.36), and PBE (12.10).**

ACM | DHDF | GGA | LDA | MAD

Obtaining chemical accuracy ( $\sim 1$  kcal/mol) to quantify key chemical quantities (e.g., heats of formation, bond dissociation energies, and reaction barrier heights) using quantum mechanics (QM) has been a major focus in the development of the theory. This has led to, for example, the Gn method (1, 2) that approaches this chemical accuracy. Because G3 is a coupled cluster based method, it scales on the order of  $N^7$ , where  $N$  measures the system size, limiting to fairly small species for routine use.

The desire to predict unique physiochemical phenomena (e.g., solvation, catalysis, self assembly, and drug design) in practical (large) systems has brought about a second major focus of the oretical development, leading, for example, to divide and conquer formulations to attain more efficient scaling (3), but with much lower accuracy than Gn.

Density functional theory (DFT) in the framework of Kohn Sham (KS) scheme (4, 5) provides a “shortcut” to the many body problem. Many density functional approximations (DFAs), provide typical scaling of  $N^3 \sim N^4$ , while yielding significantly more accurate results than Hartree Fock (HF) theory, the lowest level wave function based method with similar scaling, but they still lead to significant errors for some systems. For example, current DFAs lead to a poor description of London dispersion (van der Waals attraction), which is essential to predict the packing of molecules into solids, and the binding of drug molecules to proteins. These DFAs are also poor in predicting the magnitude of reaction barriers.

In this article, we develop and present a unique functional, XYGJ OS, that provides a good combination of high accuracy and speed. XYGJ OS involves a doubly hybrid density functional (DHDF), containing both a nonlocal orbital dependent component in the exchange term (HF like exchange), and also information about the unoccupied KS orbitals in the electron correlation part (PT2, perturbation theory up to second order) using the opposite spin (OS) ansatz to include the locality of electron correlation. XYGJ OS provides accuracy comparable to that of Gn for the test datasets and speed with  $N^2 \sim N^3$  for the local implementation. Hence XYGJ OS is both accurate and fast.

## Theory

The Holy Grail in KS DFT is to find the exact, yet unknown, exchange correlation functional  $E_{xc}[\rho]$  using density  $\rho$  as the basic variable (4, 5). In practice, an approximate  $E_{xc}$  must be adopted, which is often partitioned into the exchange and correlation parts

$$E_{xc}[\rho] \approx E_x^{DFA}[\rho] + E_c^{DFA}[\rho]. \quad [1]$$

$E_x^{DFA}$  has been extended to include a portion of nonlocal  $E_x^{HF}$ , where the superscript “HF” emphasizes that the exchange part has the same form as in Hartree Fock theory (6). The exchange correlation potential  $v_{xc}$  in the  $n$ th cycle of the self consistent field (SCF) process to solve the KS equation is obtained as a functional of  $\rho$  of the previous cycle.

On the other hand, Görling and Levy (GL) (7, 8) argued that the same KS scheme should work as well in terms of KS orbitals  $\varphi_i$  and eigenvalues  $\varepsilon_i$ . GL proposed a formally exact KS scheme based on perturbation theory, where  $E_{xc}$  was expressed as:

$$E_{xc}[\rho] = E_x^{HF}[\{\varphi_i\}] + \sum_{j=2}^{\infty} E_{c,j}[\{\varphi_i\}, \{\varepsilon_i\}, \{v_1(r), v_2(r), \dots, v_{j-1}(r)\}], \quad [2]$$

$$E_{c,2} = E_c^{GL2} = \sum_{i=1}^{\infty} \frac{|\langle \Phi_{s,0} | \hat{V}_{ee} - v_1 | \Phi_{s,i} \rangle|^2}{E_{s,0} - E_{s,i}}. \quad [3]$$

Here  $E_c^{GL2}$  stands for the GL perturbation theory up to the second order,  $\{\Phi_{s,0}, E_{s,0}\}$  and  $\{\Phi_{s,i}, E_{s,i}\}$  are the wave function and energy for the ground state and the  $i$ th excited state of an  $N$  electron KS system, respectively;  $\hat{V}_{ee}$  is the operator of electron electron repulsion, and the  $v_1$  potential may be determined from the “exchange only” KS equation (8). With knowledge of the potentials  $v_j(r)$ , Eq. 2 gives the formally exact exchange correlation energy as functional of the KS orbitals  $\varphi_i$  and eigenvalues  $\varepsilon_i$ , with which the approximate  $E_{xc}^{DFA}[\rho]$  defined in [1] can be compared. However, in practice, such a procedure is difficult to apply to higher than second order due to the unfavorable scaling with the system size, and in many cases perturbation theory is nonconvergent. Thus the scheme must be simplified to make it applicable for including higher order contributions.

Author contributions: X.X., Y.J., and W.A.G. designed research; I.Y.Z., X.X., and Y.J. performed research; I.Y.Z., X.X., Y.J., and W.A.G. analyzed data; and I.Y.Z., X.X., Y.J., and W.A.G. wrote the paper.

The authors declare no conflict of interest.

<sup>1</sup>To whom correspondence may be addressed. E-mail: xxchem@fudan.edu.cn, or ysjn@kaist.ac.kr, or wag@wag.caltech.edu.

This article contains supporting information online at [www.pnas.org/lookup/suppl/doi:10.1073/pnas.1115123108/-DCSupplemental](http://www.pnas.org/lookup/suppl/doi:10.1073/pnas.1115123108/-DCSupplemental).

The adiabatic connection method [(ACM), ref. 9, 10], which defines a family of partially interacting  $N$  electron systems with a coupling constant for a fixed  $\rho$ , provides a powerful tool for developing and understanding  $E_{xc}$  (6, 11–13). ACM suggests that Eq. 2 up to second order, while being more appropriate for coupling close to zero, is only exact if the potential energy of exchange correlation depends linearly on the coupling strength, whereas [1] is more associated with full electron electron coupling (13, also see *SI Text* for more discussion). To go beyond the linear approximation and to take advantages of both [1] and Eq. 2, we define an empirical DHDF that combines Eq. 2 ( $j = 2$ ) with [1]:

$$E_{xc}^{DHDF}[\rho] = c_1 E_x^{LDA} + c_2 \Delta E_x^{GGA} + c_3 E_x^{HF} + c_4 E_c^{LDA} + c_5 \Delta E_c^{GGA} + c_6 E_c^{PT2}. \quad [4]$$

Here  $\{E_x^{LDA}, E_c^{LDA}\}$  are the exchange and correlation components within the local density approximation (LDA), and  $\{\Delta E_x^{GGA}, \Delta E_c^{GGA}\}$  are the corresponding correction terms to LDA within the generalized gradient approximation (GGA). The meta GGA functionals that include kinetic energy density or the Laplacian of density can also be used in place of GGAs. Such a combination suggests that only the energetically most important double excitation PT2 term in Eq. 2 need be calculated explicitly, the higher order correlations are embedded into the parameterized terms such as  $(E_{xc}^{DFA} - E_x^{HF})$  (12). Other examples of DHDFs include MC3BB (14), B2PLYP (15), B2GP PLYP (16), and  $\omega$ B97X 2 (17), which are derived and constructed differently (see below and *SI Text* for more discussion).

Several key issues distinguish our approach from GL perturbation theory (7, 8) and other DHDFs (14–23).

- i. Instead of seeking for  $\{\varphi_i, \varepsilon_i, v_j\}$  self consistently and order by order via Eq. 2, we use a conventional DFA defined in [1] to generate  $\{\varphi_i, \varepsilon_i\}$  and to evaluate  $E_{xc}$  defined in Eq. 4 in a post SCF manner. In fact, the GL perturbation theory, Eq. 2, was built on KS orbitals with a local effective potential, while we have extended it to include hybrid functionals with generalized KS orbitals (12, 13).
- ii.  $E_c^{PT2}$  differs from  $E_c^{GL2}$  in that the singles contribution is not explicitly calculated, but we argue (12, 13) that it can be reasonably absorbed into the parameterization in Eq. 4. Higher order contributions  $E_{c,j}$  ( $j > 2$ ) are also implicitly included via the parameterization.
- iii. Neglecting the nonlocal exchange correlation effects ( $E_x^{HF}, E_c^{PT2}$ ) in Eq. 4 leads to a pure DFA, while neglecting the local exchange correlation effects, Eq. 4 gives an approximation to GL2. Hence our DHDF may be regarded as an interpolation approach between a pure DFA and GL2, while both of them are in the framework of the KS scheme. As different orbitals are used to construct the PT2 term, neglecting the local exchange correlation effects in other DHDFs (14–23) will bring back the conventional MP2, such that these DHDFs may be regarded as an interpolation approach between a DFA and MP2, the wave function based lowest level correlation method. These functionals go beyond the framework of the KS scheme (23).

Assuming LDA and GGA in Eq. 4 are SVWN (24, 25) and BLYP (26, 27), respectively, we previously developed XYG3 (12), a DHDF which is remarkably accurate for a wide range of systems and important chemical properties (12, 13, 28–31). Nevertheless, the PT2 term in XYG3 and other DHDFs is evaluated in a way similar to MP2:

$$E_c^{PT2} = \frac{1}{4} \sum_{ij} \sum_{ab} \frac{|\langle \varphi_i \varphi_j | \varphi_a \varphi_b \rangle - \langle \varphi_i \varphi_j | \varphi_b \varphi_a \rangle|^2}{\varepsilon_i + \varepsilon_j - \varepsilon_a - \varepsilon_b}, \quad [5]$$

where the subscripts  $(i, j)$  and  $(a, b)$  denote the occupied and unoccupied KS spin orbitals, respectively, leading to a formal scaling as  $N^5$ , as opposed to a formal scaling of  $N^4$  as in B3LYP (24–27, 32, 33). This unfavorable scaling raises an issue for the practicality to apply DHDFs to large systems.

Density fitting approximations have often been used in electronic structure theories to reduce computational expense. In the so called “resolution of the identity” RI MP2 method (34, 35), the product of occupied and virtual orbitals ( $ia$  pair) is expanded with auxiliary functions, such that numerous 4 center 2 electron integrals based on molecular orbitals (MO) are replaced by fewer 3 and 2 center integrals with cheaper transformation from atomic orbitals (AO) to MO. RI MP2 is about 5–20 times faster than conventional MP2 (36, 37). Nevertheless, RI MP2 reduces only the prefactor, it does not change the scaling. Similarly, we have RI XYG3, which retains the original accuracy but is faster for small systems with large basis sets.

Here we propose a unique OS ansatz for DHDF, that yields a balanced description of nonlocal correlation effects while considerably reducing computational time. Our OS ansatz is motivated by the observation that the most important electron correlation effects involve correlations of the OS electrons in the same orbital. The OS ansatz leads to  $N^4$  scaling (36, 37) [using auxiliary basis expansions (34, 35) and Laplace quadrature approximations (38)]. It should be emphasized that as the same spin (SS) correlation is very important in accurate description of open shell systems and magnetic properties, such contributions cannot be simply neglected. In XYGJ OS, the SS correlation effects are included within the standard DFA.

In recognition of the “nearsightedness of electron correlation” as emphasized by Kohn (39), we then build upon XYGJ OS to introduce the local approximation for the OS electron correlation by utilizing the sparsity of the RI expansion coefficients, integral matrices, and Laplace transform matrices. The local implementation of XYGJ OS scales as  $N^3$  while retaining the accuracy of the original XYGJ OS (see *SI Text* for more discussion).

Thus our proposed functional form (XYGJ OS) is

$$E_{xc}^{XYGJ\ OS}[\rho] = e_x E_x^{HF} + (1 - e_x) E_x^S + (e_{VWN} E_c^{VWN} + e_{LYP} E_c^{LYP}) + e_{PT2} E_{c,os}^{PT2}. \quad [6]$$

In Eq. 6 we normalize the HF exchange and Slater exchange (24), while eliminating the  $\Delta E_x^{GGA}$  contribution. The correlation part consists of  $E_c^{VWN}$  (25),  $E_c^{LYP}$  (27), and  $E_{c,os}^{PT2}$ , where the first term includes both the SS and OS effects while the second and third terms include only OS components. Our concept is that the combination of VWN, LYP, and PT2 OS yields a balanced description of both local and nonlocal spin dependent correlation terms. To determine the optimal four parameters in Eq. 6, we use the experimental heats of formation (HOF) data for the G3/99 set of 223 molecules (1, 2) as the training set, leading to  $\{e_x, e_{VWN}, e_{LYP}, e_{PT2}\} = \{0.7731, 0.2309, 0.2754, 0.4364\}$ .

## Results and Discussion

We emphasize that we use the fully optimized B3LYP orbitals to generate the density and to calculate each term in Eqs. 4 or 6 (12, 13, 29–31). But the choice of LDA = SVWN and GGA = BLYP in Eqs. 4 or 6, as well as using B3LYP orbitals as input, is not unique. We find that any conventional DFAs defined in [1] can also serve the same purpose, leading to similar performance, albeit with a reoptimized set of mixing parameters. In our method, we assume that our KS wave function is the zeroth order wave function in the GL perturbation theory that gives the correct ground state electron density. Instead, MC3BB is a multicoefficient method, which mixes the total energies from the conventional MP2 and a conventional DFA calculation. Hence there are two independent SCF calculations in the MC3BB type of

DHDFs, which lead to two sets of different orbitals, yielding two different densities. In MC3BB, the SCF HF orbitals are used for MP2 evaluation (14), while it is well known that HF wave function is the one determinantal wave function which gives the lowest expectation value with the fully interacting Hamiltonian. It has been shown recently (23) that the B2PLYP family of functionals works in a way which is technically similar to MP2. These functionals adopt orbitals that minimize the one determinantal wave function based on the so called density scaled one parameter hybrid approximation. Hence, the density from the B2PLYP type of functionals is by construction not meant to be the true density. In contrast to what was originally proposed (15), there is no singles' contribution by construction in the B2PLYP family of functionals, and its theoretical basis is provided by the multidefinant extension of the Kohn Sham scheme (23). On the other hand, the key idea of the XYG3 type of functionals is to combine the GL perturbation theory and the standard KS scheme in the framework of ACM. In XYG3, only the energetically most important double excitation PT2 term in Eq. 2 is calculated explicitly using orbitals generated from a conventional DFA in [1]. Our present OS ansatz further reduces the computational cost by only calculating the most important electron correlation effects contributed by the OS electrons in the same orbital. XYGJ OS presents a unique combination of speed and accuracy. Hence, we propose that the current DHDFs shall be categorized into three types (13), as represented by MC3BB (14), B2PLYP (15), and XYG3 (12). The former two go beyond the KS scheme.

It is possible to carry out a SCF calculation for any orbital dependent  $E_{xc}$  using, for example, the direct optimization approach to compute the optimized effective potential (OEP) as proposed by Yang and coworkers (40). It was found that such a SCF procedure can often lead to unphysically unbound state with too low total energy mainly due to the near degeneracy of the orbitals in the single excitation terms. This unbound issue can be largely remedied by calculating only the double excitation terms in the post SCF manner (40). This procedure is indeed the calculation approach adopted by the XYG3 type of functionals. Furthermore, we note that extra terms will appear when formu-

lating the analytical gradients for doing geometry optimization with our functionals, which, however, will not impose any practical difficulty in implementation as compared to other types of DHDFs.

We find that XYGJ OS is remarkably accurate for a broad range of systems and important chemical properties (1, 2, 41–45) other than HOF which are *not used in fitting the parameters*. Table 1 (more details are in *SI Text*) compares the overall performance of some representative DFT methods, showing that XYGJ OS is the best or nearly best for essentially all properties, leading to chemical accuracy (1.28 kcal/mol) comparable to the G3 theory (which contains four empirical parameters involving the number of electron pairs) (1.06) and much better than MP2 (7.49 kcal/mol).

**Heats of Formation.** The 223 molecule G3/99 set (1, 2) provides a test of accuracy for the main group covalent systems. XYGJ OS gives mean absolute deviation (MAD) of 1.65 kcal/mol, lying between those of G2 (1.89) and G3 (1.06) theories. Note that the MADs for HOF listed in Table 1 associated with XYG3, B2PLYP, B2PLYP D, and  $\omega$ B97X 2(LP) are taken from the original refs. 12, 17, 22, which were obtained by using the way these functionals were parameterized. It was shown that HOF calculations with DHDFs are most prone to the basis set effects (29). The results with the G3Large basis set (1) used for optimization of the XYGJ OS functional can be found in *SI Text*, where severe basis set dependences are clearly shown.

**Charged Species.** Charged species are not included in our training set. The G2 1 set (2) for ionization potential (IP) contains 14 atoms and 24 molecules. XYGJ OS gives a MAD of 1.23 kcal/mol, being one of the best DFT methods for calculating IP. Over the 25 cases in the G2 1 set for electron affinity (EA) (2), XYGJ OS leads to MAD = 1.97 kcal/mol. Generally, increasing the size of the basis set will increase the accuracy for EA calculation with DHDFs. For the eight systems for proton affinity in the G2 and G3 sets (1), XYGJ OS leads to MAD = 1.68 kcal/mol, comparable to the performance of conventional DFAs.

**Table 1. MAD, (in kcal/mol) for various benchmarks**

Methods	HOF (223)	IP (38)	EA (25)	PA (8)	BDE (92)	NHTBH (38)	HTBH (38)	NCIE (31)	All (493)	Time*	
										C <sub>100</sub> H <sub>202</sub>	C <sub>100</sub> H <sub>100</sub>
<i>DFT methods</i>											
SVWN (LDA)	130.88	15.14	17.30	5.68	18.14	12.53	17.95	3.29	67.28		
BLYP	10.16	6.02	2.47	1.75	7.00	8.29	7.68	1.49	7.84		
PBE	20.71	5.13	2.40	1.56	3.91	8.57	9.48	1.17	12.10		
TPSS	5.01	5.36	2.41	1.66	5.88	9.04	8.26	1.14	5.33		
B3LYP	6.08	3.74	2.45	1.40	5.51	4.84	4.26	0.98	4.98	2.8	12.3
B3LYP D3	4.15	3.77	2.47	1.18	4.29	5.17	4.97	0.64	3.93		
PBE0	5.64	3.84	2.97	1.25	3.67	3.56	4.38	0.71	4.36		
M06 2X	2.26	2.72	2.37	1.94	1.40	1.26	1.25	0.28	1.86		
XYG3 <sup>†</sup>	1.81	1.31	1.84	1.61	1.57	1.29	0.75	0.32	1.51	200.0	81.4
<b>XYGJ OS</b>	<b>1.65</b>	<b>1.23</b>	<b>1.97</b>	<b>1.68</b>	<b>0.71</b>	<b>1.18</b>	<b>0.88</b>	<b>0.35</b>	<b>1.28</b>	<b>7.8</b>	<b>46.4</b>
MC3BB	3.28	2.78	4.01	1.03	2.43	1.44	0.80	0.58	2.58		
B2PLYP <sup>‡</sup>	2.74	2.48	2.15	1.52	2.95	2.23	1.73	0.55	2.45		
B2PLYP D <sup>‡</sup>	1.67	2.48	2.15	1.34	2.27	2.47	2.11	0.45	1.88		
$\omega$ B97X 2(LP) <sup>§</sup>	1.52	1.73	1.56	1.09	1.62	1.67	0.74	0.47	1.44		
<i>Wavefunction based methods</i>											
HF	213.42	23.19	26.46	3.09	32.70	9.08	13.51	2.37	107.71		
MP2	10.63	3.49	3.59	2.13	7.73	5.42	3.91	0.60	7.49		
G2	1.89	0.97	1.31	1.34	1.80	0.97	1.24	0.57	1.56		
G3	1.06	1.27	1.13	1.06	1.08	0.97	1.24	0.57	1.06		

HOF is heat of formation (1, 2), IP is ionization potential (2), EA is electron affinity (2), PA is proton affinity (2), BDE is bond dissociation energy (40), NHTBH and HTBH are barrier heights for reactions (42, 43), NCIE is the binding in molecular clusters (42, 43). The basis sets used for final energetics are G3Large unless otherwise stated. See *SI Text* for computational details.

\*The time is single CPU hours on 2.5 GHz Xeon for linear alkane C<sub>100</sub>H<sub>202</sub> and the C<sub>100</sub>H<sub>100</sub> diamond structure. The basis sets used are cc pVDZ.

<sup>†</sup>Taken from ref. 12 with 6 311+G(3df,2p).

<sup>‡</sup>HOF are taken from ref. 22 with very large basis set of CQZV3P. BDEs are calculated using the corresponding HOF.

<sup>§</sup>Taken from ref. 17 or calculated with 6 311++G(3df,3pd). BSSE corrections are included for the NCIE set.

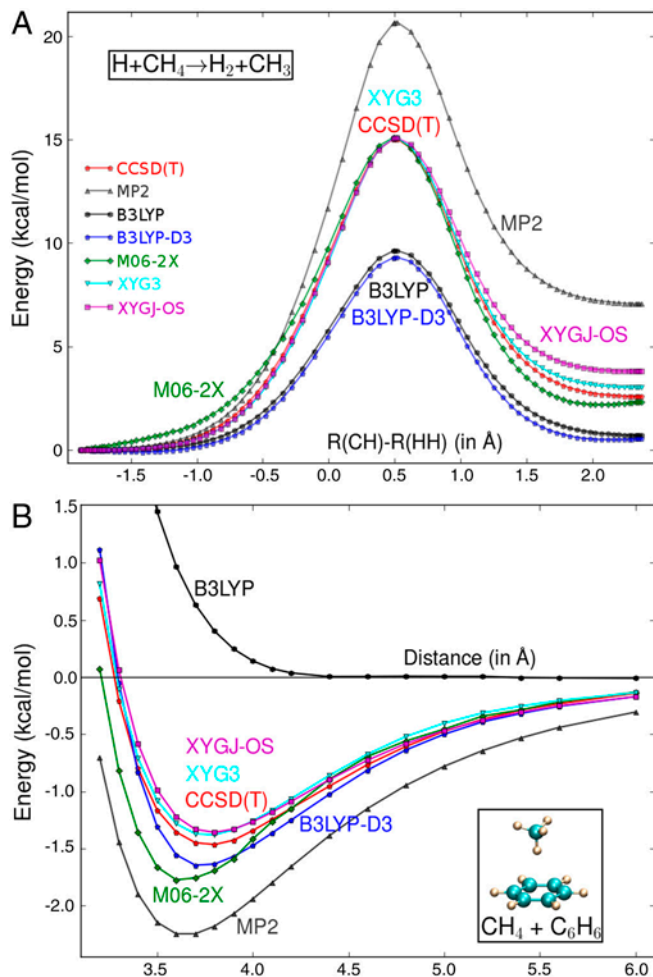


**Fig. 1.** (A) Potential energy curves for  $\text{H} + \text{CH}_4 \rightarrow \text{H}_2 + \text{CH}_3$  reaction along the reaction coordinate of  $[\text{R}(\text{CH})-\text{R}(\text{HH})]$  (in Å). (B) Intermolecular potentials for  $\text{CH}_4-\text{C}_6\text{H}_6$  complex. R is the distance from the carbon of  $\text{CH}_4$  to the ring center of  $\text{C}_6\text{H}_6$ .

**Bond Dissociation Enthalpy (BDE).** BDE is arguably the most important property for chemistry, carrying additional information other than HOFs (13). XYGJ OS leads to  $\text{MAD} = 0.71$  kcal/mol for the 92 reactions in the BDE92/07 set (40)! This accuracy surpasses the MAD of the most accurate ab initio methods, G2 (1.80) and G3 (1.09 kcal/mol). Indeed XYGJ OS leads to half the MAD of XYG3 (1.57 kcal/mol), providing strong support for the OS ansatz and the local approximation.

**Reaction Barrier Height (RBH).** We use the NHTBH and HTBH datasets of Zhao and Truhlar as testing sets (42, 43) of RBHs. NHTBH contains six heavy atom transfer reactions, eight nucleophilic substitution reactions, five unimolecular and association reactions, while HTBH comprises solely 19 hydrogen transfer reactions. XYGJ OS leads to  $\text{MAD} = 1.03$  kcal/mol for the two sets together, a significant improvement over B3LYP (4.55 kcal/mol) and MP2 (4.67 kcal/mol). Note that the dispersion corrected methods [e.g., B3LYP D3 (46)] may deteriorate the performance for RBH calculations.

We test various methods in describing the whole  $\text{H} + \text{CH}_4 \rightarrow \text{H}_2 + \text{CH}_3$  reaction path using the coupled cluster method with

single and double as well as perturbative triple excitations (CCSD)(T)/6-311++G(3df,2pd) data (43) as the reference. The results are depicted in Fig. 1A. XYGJ OS results are nearly identical to the XYG3 and CCSD(T) results before the barrier. But XYGJ OS overestimates the reaction endothermicity by 1.21 kcal/mol.

**Nonbonded Interaction (NBI).** We use the NCIE dataset of Zhao and Truhlar (42, 43) to test the XYGJ OS performance for the description of NBIs. The NCIE set includes six hydrogen bond complexes, seven charge transfer complexes, six dipole interaction complexes, seven weak interaction complexes, and five  $\pi-\pi$  stacking complexes. XYGJ OS ( $\text{MAD} = 0.35$  kcal/mol) does quite well for NBI, including the London dispersion dominant systems in the NCIE dataset. For the S22 set (47), which contains larger molecules (e.g., uracil dimer, adenine thymine complexes) that are more biologically related, XYGJ OS ( $\text{MAD} = 0.36$  kcal/mol) leads to similar accuracy as the dispersion corrected methods (22, 46). On average, B3LYP D3 improves B3LYP by 0.34 kcal/mol for the NCIE set. While significant improvements occur for the weak interaction complexes, and the  $\pi-\pi$  stacking complexes, B3LYP D3 significantly overbinds the hydrogen bond complexes, and the charge transfer complexes (see *SI Text* for more discussion).

We test various methods in describing the intermolecular potentials of the  $\text{CH}_4-\text{C}_6\text{H}_6$  complex calculated by various methods. The CCSD(T) results at the complete basis set (CBS) limit are used as reference (44). As shown in Fig. 1B, XYGJ OS data are nearly on top of those of XYG3.

**Scaling.** Equally important is that XYG3 and other DHDFs (15 19) scale formally with the fifth power of the size, while XYGJ OS scales formally with the fourth power, and for the local implementation it scales formally with the third power. In contrast, the most accurate ab initio methods, CCSD(T), and G3, scale as the seventh power. Indeed, Table 1 shows that the total computational time for  $\text{C}_{100}$  chains and diamondoids with local XYGJ OS is just 3 to 4 times that for B3LYP (a part of XYGJ OS), with a scaling of  $N^{2.1}$  for n alkanes (See *SI Text* for more details).

## Summary

We have developed and validated here a unique doubly hybrid density functional, XYGJ OS, using Walter Kohn's insight about "nearsightedness" of electron correlation by including explicitly only the correlation between electrons of OS and then only the parts that are in the same region of space. We show that XYGJ OS achieves nearly chemical accuracy (1.28 kcal/mol) with computational costs scaling as  $N^3$ . This unique combination of high accuracy and speed leads to a practical level of calculation while attaining chemical accuracy for large molecular systems.

**ACKNOWLEDGMENTS.** X.X. acknowledges the support of NSF of China (91027044, 21133004, 20923004), and the Ministry of Science and Technology of China (2007CB815206, 2011CB808505). Y.J. acknowledges the support of National Research Foundation (NRF) of Korea (2010 0023018, 2010 0029034, and 2010 0029728) by the Ministry of Education, Science and Technology (MEST) of Korea. W.A.G. acknowledges the support of USA National Science Foundation (NSF) (ECS 0609128, CTS 0608889), the Center for Catalytic Hydrocarbon Functionalization (Department of Energy, Basic Energy Sciences Award DE SC0001298), and Office of Naval Research Defense Advanced Research Projects Agency [ONR DARPA (PROM N00014 06 1 0938 and N00014 05 1 0778)]. Y.J. and W.A.G. have also been supported by the World Class University (WCU) (NRF R 31 2008 000 10055 0) program funded by the Ministry of Education, Science and Technology.

- Curtiss LA, Redfern PC, Raghavachari K, Pople JA (2001) Gaussian-3X (G3X) theory: use of improved geometries, zero-point energies, and Hartree-Fock basis sets. *J Chem Phys* 114:108–117.
- Curtiss LA, Redfern PC, Raghavachari K, Pople JA (1998) Assessment of Gaussian-2 and density functional theories for the computation of ionization potentials and electron affinities. *J Chem Phys* 109:42–55.

- Yang WT (1991) Direct calculation of electron density in density-functional theory. *Phys Rev Lett* 66:1438–1441.
- Hohenberg P, Kohn W (1964) Inhomogeneous electron gas. *Phys Rev B* 3:864–871.
- Kohn W, Sham LJ (1965) Self-consistent equations including exchange and correlation effects. *Phys Rev A* 4:1133–1138.

6. Becke AD (1993) A new mixing of Hartree-Fock and local density-functional theories. *J Chem Phys* 98:1372–1377.
7. Görling A, Levy M (1993) Correlation-energy functional and its high-density limit obtained from a coupling-constant perturbation expansion. *Phys Rev B* 47:13105–13113.
8. Görling A, Levy M (1994) Exact Kohn-Sham scheme based on perturbation theory. *Phys Rev A* 50:196–204.
9. Langreth DC, Perdew JP (1977) Exchange-correlation energy of a metallic surface: wave-vector analysis. *Phys Rev B* 15:2884–2902.
10. Gunnarsson O, Lundqvist B (1976) Exchange and correlation in atoms, molecules, and solids by the spin-density-functional formalism. *Phys Rev B* 13:4274–4298.
11. Mori-Sanchez P, Cohen AJ, Yang WT (2006) Self-interaction-free exchange-correlation functional for thermochemistry and kinetics. *J Chem Phys* 124:1–4.
12. Zhang Y, Xu X, Goddard W A, III (2009) Doubly hybrid density functional for accurate description of nonbond interactions, thermochemistry, and thermochemical kinetics. *Proc Natl Acad Sci USA* 106:4963–4968.
13. Zhang IY, Xu X (2011) Doubly hybrid density functional for accurate description of thermochemistry, thermochemical kinetics and nonbonded interactions. *Int Rev Phys Chem* 46:115–160.
14. Zhao Y, Lynch BJ, Truhlar DG (2004) Doubly hybrid meta DFT: new multi-coefficient correlation and density functional methods for thermochemistry and thermochemical kinetics. *J Phys Chem A* 108:4786–4791.
15. Grimme S (2006) Semiempirical hybrid density functional with perturbative second-order correlation. *J Chem Phys* 124:1–16.
16. Karton A, Tarnopolsky A, Lamère J-F, Schatz GC, Martin JML (2008) Highly accurate first-principles benchmark datasets for the parametrization and validation of density functional and other approximate methods Derivation of a robust, generally applicable, double-hybrid functional for thermochemistry and thermochemical kinetics. *J Phys Chem A* 112:12868–12886.
17. Chai JD, Head-Gordon M (2009) Long-range corrected double-hybrid density functionals. *J Chem Phys* 131:1–13.
18. Sancho-García JC, Pérez-Jiménez AJ (2009) Assessment of double-hybrid energy functionals for  $\pi$ -conjugated systems. *J Chem Phys* 131:1–11.
19. Graham DC, Menon AS, Goerigk L, Grimme S, Radom L (2009) Optimization and basis-set dependence of a restricted-open-shell form of B2-PLYP double-hybrid density functional theory. *J Phys Chem A* 113:9861–9873.
20. Benighaus T, DiStasio RA, Lochan R, Chai JD, Head-Gordon M (2008) Semiempirical double-hybrid density functional with improved description of long-range correlation. *J Phys Chem A* 112:2702–2712.
21. Schwabe T, Grimme S (2006) Towards chemical accuracy for the thermodynamics of large molecules: new hybrid density functionals including non-local correlation effect. *Phys Chem Chem Phys* 8:4398–4401.
22. Schwabe T, Grimme S (2007) Double-hybrid density functionals with long-range dispersion corrections: higher accuracy and extended applicability. *Phys Chem Chem Phys* 9:3397–3406.
23. Sharkas K, Toulouse J, Savin A (2011) Double-hybrid density-functional theory made rigorous. *J Chem Phys* 134:1–9.
24. Dirac PAM (1930) Note on exchange phenomena in the Thomas atom. *Math Proc Cambridge* 26:376–385.
25. Vosko SH, Wilk L, Nusair M (1980) Accurate spin-dependent electron liquid correlation energies for local spin density calculations: a critical analysis. *Can J Phys* 58:1200–1211.
26. Becke AD (1988) Density-functional exchange-energy approximation with correct asymptotic behavior. *Phys Rev A* 38:3098–3100.
27. Lee C, Yang W, Parr RG (1988) Development of the Colle-Salvetti correlation-energy formula into a functional of the electron density. *Phys Rev B* 37:785–789.
28. Zhang IY, Luo Y, Xu X (2010) XYG3s: speedup of the XYG3 fifth-rung density functional with scaling-all-correlation method. *J Chem Phys* 132:1–11.
29. Zhang IY, Luo Y, Xu X (2010) Basis set dependence of the doubly hybrid XYG3 functional. *J Chem Phys* 133:1–12.
30. Zhang IY, Wu JM, Luo Y, Xu X (2010) Trends in R-X bond dissociation energies ( $R^{\bullet}$  = Me, Et, *i*-Pr, *t*-Bu,  $X^{\bullet}$  = H, Me, Cl, OH). *J Chem Theory Comput* 6:1462–1469.
31. Zhang IY, Wu JM, Xu X (2010) Extending the reliability and applicability of B3LYP. *Chem Commun* 46:3057–3070.
32. Becke AD (1993) Density-functional thermochemistry III. The role of exact exchange. *J Chem Phys* 98:5648–5652.
33. Stephens PJ, Devlin FJ, Chabalowski CF, Frisch MJ (1994) Ab initio calculation of vibrational absorption and circular dichroism spectra using density functional force fields. *J Phys Chem* 98:11623–11627.
34. Feyereisen M, Fitzgerald G, Komornicki A (1993) Use of approximate integrals in ab initio theory. An application in MP2 energy calculations. *Chem Phys Lett* 208:359–363.
35. Weigend F, Haser M, Patzelt H, Ahlrichs R (1998) RI-MP2: optimized auxiliary basis sets and demonstration of efficiency. *Chem Phys Lett* 294:143–152.
36. Jung YS, Lochan RC, Dutoi AD, Head-Gordon M (2004) Scaled opposite-spin second order Møller-Plesset correlation energy: an economical electronic structure method. *J Chem Phys* 121:9793–9802.
37. Jung YS, Shao YH, Head-Gordon M (2007) Fast evaluation of scaled opposite spin second-order Møller-Plesset correlation energies using auxiliary basis expansions and exploiting sparsity. *J Comput Chem* 28:1953–1964.
38. Almlöf J (1991) Elimination of energy denominators in Møller-Plesset perturbation theory by a Laplace transform approach. *Chem Phys Lett* 181:319–320.
39. Kohn W (1996) Density functional and density matrix method scaling linearly with the number of atoms. *Phys Rev Lett* 76:3168–3171.
40. Mori-Sánchez P, Wu Q, Yang WT (2005) Orbital-dependent correlation energy in density-functional theory based on a second-order perturbation approach: success and failure. *J Chem Phys* 123:1–14.
41. Wu JM, Xu X (2007) The X1 method for accurate and efficient prediction of heats of formation. *J Chem Phys* 127:1–8.
42. Zhao Y, Truhlar DG (2008) Density functionals with broad applicability in chemistry. *Theor Chem Acc* 120:215–241.
43. Zhao Y, Truhlar DG (2005) Design of density functionals that are broadly accurate for thermochemistry, thermochemical kinetics, and nonbonded interactions. *J Phys Chem A* 109:5656–5667.
44. Zhang LL, Lu YP, Lee S-Y, Zhang DH (2007) A transition state wave packet study of the  $H + CH_4$  reaction. *J Chem Phys* 127:1–7.
45. Takatani T, Sherrill CD (2007) Performance of spin-component-scaled Møller-Plesset theory (SCS-MP2) for potential energy curves of noncovalent interactions. *Phys Chem Chem Phys* 9:6106–6114.
46. Grimme S, Antony J, Ehrlich S, Krieg H (2010) A consistent and accurate ab initio parametrization of density functional dispersion correction (DFT-D) for the 94 elements H-Pu. *J Chem Phys* 132:1–19.
47. Jurecka P, Sponer J, Cerny J, Hobza P (2006) Benchmark database of accurate (MP2 and CCSD(T) complete basis set limit) interaction energies of small model complexes, DNA base pairs, and amino acid pairs. *Phys Chem Chem Phys* 8:1985–1993.

# Supporting Information

Zhang et al. 10.1073/pnas.1115123108

## SI Text

**Computational Details and Accuracy Test Database.** Perdew has formulated the hierarchy of density functional theory (DFT) approximations as a “Jacob’s ladder” rising from the “earth of Hartree” to the “heaven of chemical accuracy” (1). We tested here the performance of some representative functionals of each rung (2–23). These functionals are the first rung: SVWN (2, 3); the second rung: BLYP (4, 5), PW91 (6, 7), PBE (8); the third rung: M06 L (9), TPSS (10); the fourth rung: B3LYP (4, 5, 11–13), X3LYP (14), PBE0 (15), M06 2X (16), M06 (16); and the fifth rung: XYG3 (17), XYGJ OS, MC3BB (18), B2PLYP (19), B2GP LYP (20), and  $\omega$ B97X 2(LP) (21). The corresponding dispersion corrected methods: B3LYP D (22), B3LYP D3 (23), and B2PLYP D (22) are also tested.

Single point DFT calculations were performed with the G3Large basis set (24) for heats of formation (HOFs), ionization potentials (IPs), electron affinities (EAs), proton affinities (PAs), bond dissociation enthalpies (BDEs), reaction barrier heights (RBHs), and nonbonded interactions (NBIs). Only HOFs of the G3/99 set (24–26) were used as the training set to optimize the parameters in XYG3 and XYGJ OS. All other data were used as the testing sets. The results are summarized in Table S1.

For HOFs (at 298 K and 1 atm), the G3/99 set (24–26) was used as reference. The geometries were optimized using B3LYP with the 6 31G(2df,p) basis set. Analytical vibrational frequencies were calculated at the same level and scaled by 0.9854 to estimate zero point energies and thermo corrections. The same strategy is used in the G3X method (24). Spin orbit corrections were included as in the Gn method (24–26). HOFs were calculated via atomization procedure.

For IPs, EAs, and PAs (at 0 K), the G2 1 set (24–26) was used as reference. These properties were calculated as energy differences between the neutral species and the corresponding ionic species. As in the Gn method (24–26), the geometries were optimized using MP2(full) with the 6 31G(d) basis set. Analytical vibrational frequencies were calculated at the level of HF/6 31G(d) and scaled by 0.8929 to estimate zero point energies.

For BDEs, the BDE92/07 set (27) was used as reference. BDEs were calculated according to the enthalpy change of the following reaction in the gas phase at 298 K and 1 atm:

$$X - Y(g) = X \cdot (g) + Y \cdot (g),$$

$$BDE(X - Y) = \Delta_f H_{298}^\circ(X \cdot) + \Delta_f H_{298}^\circ(Y \cdot) - \Delta_f H_{298}^\circ(X - Y).$$

For RBHs, Truhlar’s nonhydrogen transfer barrier height (NHTBH) set and hydrogen transfer barrier height (HTBH) set were used as reference. The geometries are taken from Truhlar database website (28, 29).

For NBIs, Truhlar’s noncovalent interaction energy (NCIE) set was used as reference. The geometries are taken from Truhlar database website (29).

We also included some wave function based methods: HF, MP2, SCS MP2 (30), SOS MP2 (31) for comparison. Composite methods such as G2 and G3 (24–26) were used as references. Geometries and thermo corrections were all done using the standard procedure built in the Gn method. For RBHs and NBIs, the Gn results are replaced with QCISD(T)/6 311+G(3df,2p) ones, where the geometries are taken from Truhlar database website (28, 29).

The performances of various methods are summarized as follows (see Table S1).

We tested various methods in describing the whole  $H + CH_4 \rightarrow H_2 + CH_3$  reaction path using CCSD(T)/6 311+G(3df,2pd) data (32) as the reference. The results are depicted in Fig. S1. XYGJ OS results are nearly identical to the XYG3 and CCSD(T) results before the barrier. But XYGJ OS overestimates the reaction endothermicity by 1.21 kcal/mol. Note that RBH are not included in the training set of XYG3 and XYGJ OS.

We tested various methods in describing the intermolecular potentials of the  $CH_4 \cdots C_6H_6$  complex calculated by various methods as shown in Fig. S2. The CCSD(T) results at the complete basis set (CBS) limit are used as reference (33). An unpruned (250,590) grid is used in calculations to avoid spurious oscillations on potential energy curves for dispersion bound complexes with MC3BB and the M06 family of functionals (34). As shown in Fig. S2, XYGJ OS data are nearly on top of those of XYG3. Note that nonbonded interaction is not included in the training set of XYG3 and XYGJ OS. However we do not include BSSE corrections with XYG3 and XYGJ OS in comparing to the G3 and M06 data bases.

The total CPU timings are compared for XYG3 RI, XYGJ OS, and local XYGJ OS (see Fig. S3). We used *n* alkanes as examples. The calculations were performed with cc pVDZ basis sets with the same basis set as the auxiliary basis. The numbers of basis functions are 250 for  $C_{10}$ , 1,210 for  $C_{50}$ , and up to 2,410 for  $C_{100}$ . For local XYGJ OS, a cutoff criterion of  $5 \times 10^{-6}$  for local screening and the  $\omega$  value of 0.2 a.u. for the attenuated Coulomb fitting metric (Eq. S17 below) were used (35). As compared to XYGJ OS, the local algorithm errors for total energies of *n* alkanes are less than 0.01 eV (0.25 kcal/mol) up to  $C_{100}$ . For the atomization energies of G2 set, we obtained the same statistical results (less than 0.001 eV of difference) for both XYGJ OS and its local version.

The  $\omega$ B97X 2(LP) results are taken from ref. 21. The  $\omega$ B97X 2(LP) yields a very high accuracy comparable to XYGJ OS for HOF, IP, EA, PA, NHTBH, and HTBH, where the key difference in terms of accuracy is that, in  $\omega$ B97X 2(LP) all the latter properties were part of the training set used in the fitting process while in XYGJ OS only the HOF was used as a training set. XYGJ OS contains four fitting parameters while parameters in Becke88 exchange and LYP correlation functionals are fixed at their original values. The  $\omega$ B97X 2(LP) contains 16 fitting parameters. Another difference is that, the parameters in the  $\omega$ B97X 2(LP) were fitted assuming the large Pople basis 6 311+G(3df,3pd). There is also a computational difference between  $\omega$ B97X 2 ( $N^5$ ) and XYGJ OS ( $N^3$  for the default local implementation and  $N^4$  for canonical).

From Table S1, it is clear that HOF calculations are very basis set dependent, where the calculations with the basis sets used for DHDF functional parameterization lead to the best results. Changing basis sets from 6 311+G(3df,2p) to G3Large increases XYG3 MAD for HOF by 1.63 kcal/mol. Changing basis sets from CQZV3P (quadruple basis sets plus three set of polarization and core polarization functions) to G3Large increases B2PLYP MAD by 4.85 kcal/mol and B2PLYP D MAD by 4.22 kcal/mol. Changing basis sets from 6 311+G(3df,3pd) to G3Large increases  $\omega$ B97X 2(LP) MAD for HOF by 3.82 kcal/mol. For other properties, basis set dependence associated with DHDFs is relatively mild.

Dispersion correction methods could increase the errors for RBH and hydrogen bond interactions, but they should significantly improve the performance for systems (clusters) dominated by weak (vdw) interactions. Thus for RBH (Truhlar datasets

NHTBH38 and HTBH38 in Table S2), we find MAD = 4.47 kcal/mol (B3LYP), 5.12 (B3LYP D) and 4.98 (B3LYP D3). Grimme, et al. (57) found MAD = 4.7 (B3LYP), 5.4 (B3LYP D) and 5.2 kcal/mol (B3LYP D3), which are slightly different due to differences in the basis sets. For nonbonded interactions (Truhlar dataset NCIE31 in Table S3), we find MAD = 0.95 kcal/mol (B3LYP), 0.71 (B3LYP D), and 0.70 (B3LYP D3). In fact, B3LYP is much worse for the  $\pi$   $\pi$  stacking complexes than these numbers suggest, because we assess the error at the correct geometry. B3LYP D and D3 give correct geometry and lead to decreased error. On the other hand, for the hydrogen bond and charge transfer complexes, the agreement is worse for the dispersion corrected methods.

All calculations reported in this article were performed using a development version of Q Chem (36).

**XYG3 vs. XYGJ-OS.** In this section of SI, we summarize some basic physics associated with XYG3 and XYGJ OS. The way of deviation of XYG3 and XYGJ OS presented here complements that in the main text.

The Holy Grail in Kohn Sham (KS) DFT is to find the exact, yet unknown, exchange correlation functional  $E_{xc}[\rho]$  using density  $\rho$  as the basic variable (37–39). The density functional approximation (DFA) often partitions  $E_{xc}$  into exchange and correlation parts

$$E_{xc}[\rho] \approx E_x^{\text{DFA}}[\rho] + E_c^{\text{DFA}}[\rho]. \quad [\text{S1}]$$

Various approximations to this divine functional have been developed and tested in recent decades, but the accuracy of the best methods practical for important applications is often not adequate.

The adiabatic connection approach provides a powerful tool for developing and understanding  $E_{xc}$  (40, 41). This approach defines a family of partially interacting  $N$  electron systems for a fixed  $\rho$ ,

$$\hat{H}_\lambda = \hat{T} + \hat{V}_{\text{ee},\lambda} + \hat{V}_{\text{ext},\lambda} = \hat{T} + \lambda \hat{V}_{\text{ee}} + \sum_i^N v_\lambda(r_i), \quad [\text{S2}]$$

where both the two electron operator  $\hat{V}_{\text{ee}} = \sum_{i<j}^N 1/r_{ij}$  and the external potential depends upon the coupling strength  $\lambda$ . Here  $\lambda = 0$  corresponds to the noninteracting KS system with  $\hat{H}_s$ , while  $\lambda = 1$  leads to the physical system.  $E_{xc}$  is then given by (40, 41):

$$E_{xc}[\rho] = \int_0^1 U_{xc,\lambda}[\rho] d\lambda, \quad [\text{S3}]$$

where  $U_{xc,\lambda}$  is the potential energy of exchange correlation at intermediate coupling strength  $\lambda$ . Regrettably, the exact integrand  $U_{xc,\lambda}$  is unknown. Eq. S2 may be reformulated as

$$\hat{H}_\lambda = \hat{H}_s + \lambda \hat{H}'_\lambda, \quad [\text{S4}]$$

where the perturbation term is given by

$$\hat{H}'_\lambda = \hat{V}_{\text{ee}} + \frac{1}{\lambda} \sum_i^N \left[ v_\lambda(r_i) - v_s(r_i) \right]. \quad [\text{S5}]$$

From perturbation theory and relations based on uniform coordinate scaling (42), we obtain

$$U_{xc,\lambda} = E_x^{\text{HF}} + 2\lambda E_c^{\text{GL2}} + O(\lambda^2). \quad [\text{S6}]$$

Here  $E_c^{\text{GL2}}$  is the Görling Levy theory of coupling constant perurbation expansion to second order (43):

$$E_c^{\text{GL2}} = \sum_i \sum_a \frac{|\langle \varphi_i | v_x - \hat{k}_x | \varphi_a \rangle|^2}{\varepsilon_i - \varepsilon_a} + \frac{1}{4} \sum_{ij} \sum_{ab} \frac{|\langle \varphi_i \varphi_j | \varphi_a \varphi_b \rangle - \langle \varphi_i \varphi_j | \varphi_b \varphi_a \rangle|^2}{\varepsilon_i + \varepsilon_j - \varepsilon_a - \varepsilon_b}, \quad [\text{S7}]$$

where subscripts ( $i, j$ ) denote occupied KS orbitals, and ( $a, b$ ) denote virtual orbitals. Here  $v_x$  is the local exchange operator defined by the exchange part of Eq. S8,

$$v_{xc}(r) = \frac{\delta E_{xc}[\rho]}{\delta \rho}, \quad [\text{S8}]$$

while  $\hat{k}_x$  in Eq. S7 is the Fock like nonlocal exchange operator, leading to  $E_x^{\text{HF}}$ :

$$E_x^{\text{HF}} = -\frac{1}{2} \sum_{ij} \iint d^3r' d^3r \frac{\varphi_i^*(r) \varphi_j(r) \varphi_j^*(r') \varphi_i(r')}{|r' - r|}. \quad [\text{S9}]$$

The superscript “HF” emphasizes that it has the same form as in Hartree Fock (HF) theory. Eq. S9 is exact if the KS orbitals give the true density. Inserting Eq. S6 into Eq. S3 leads to:

$$E_{xc}[\rho] \approx E_x^{\text{HF}}[\{\varphi_i[\rho]\}] + E_c^{\text{GL2}}[\{\varphi_i[\rho]\}]. \quad [\text{S10}]$$

If  $U_{xc,\lambda}$  depends linearly on  $\lambda$ , the higher order term  $O(\lambda^2)$  in Eq. S6 is zero, such that the higher order term  $O(\lambda^3)$  in [S10] vanishes; i.e., [S10] provides an exact expression in this condition. The  $\{\varphi[\rho]\}$  indicates an orbital dependent functional. For practical uses, one needs an  $E_{xc}^{\text{DFA}}[\rho]$  that generates good KS orbitals (17, 44, 45, 46).

To improve the linear approximation of  $U_{xc,\lambda}$ , we define a doubly hybrid density functional (DHDF) that combines [S10] and [S1]:

$$E_{xc}^{\text{DHDF}}[\rho] = c_1 E_x^{\text{LDA}} + c_2 \Delta E_x^{\text{GGA}} + c_3 E_x^{\text{HF}} + c_4 E_c^{\text{LDA}} + c_5 \Delta E_c^{\text{GGA}} + c_6 E_c^{\text{GL2}}. \quad [\text{S11}]$$

Here  $\{E_x^{\text{LDA}}, E_c^{\text{LDA}}\}$  are the exchange and correlation components within the local density approximation (LDA), and  $\{\Delta E_x^{\text{GGA}}, \Delta E_c^{\text{GGA}}\}$  are the corresponding correction terms to LDA within the generalized gradient approximation (GGA). The meta GGA functionals that include kinetic energy density or the Laplacian of density can also be used in replace of GGAs. [S10] is more appropriate near  $\lambda = 0$ , while [S1] is more appropriate near  $\lambda = 1$ . Therefore Eq. S11 combines both to embrace local and nonlocal parts of both exchange and correlation contributions, which we expect to provide a good form for general applications. MC3BB (18), B2PLYP (19) and  $\omega$ B97X 2 (21), which are derived and constructed differently, are examples of other doubly hybrid functionals (18–21, 47–49). Neglecting the nonlocal correlation effects, Eq. S11 leads to such conventional hybrid functionals as Becke’s half and half (50) and B3LYP (12).

Based on Eq. S11, we have developed a DHDF, namely XYG3 (17), which is remarkably accurate for a wide range of systems and important chemical properties (17, 44, 45, 46). Nevertheless, including the PT2 term in DHDFs (17–21) leads to a formal scaling as  $N^5$ , as opposed to a formal scaling of  $N^4$  as in B3LYP. This unfavorable scaling raises an issue for the practicality to apply XYG3 to large systems.

Here we propose a new opposite spin (OS) ansatz for DHDF, namely XYGJ OS, that yields a balanced description of nonlocal correlation effects while considerably reducing computational time. Our OS ansatz is motivated by the observation that the most important electron correlation effects involves correlation of the

OS electrons in the same orbital. The OS ansatz leads to  $N^4$  scaling [using auxiliary basis expansions and Laplace quadrature approximations (31, 35)]. In XYGJ OS, the same spin (SS) correlation effects are included within the standard DFA. A local version of XYGJ OS is further developed that introduces the local approximation for the OS electron correlation. Local XYGJ OS scales as  $N^3$  by recognizing the “nearsightedness of electron correlation” as emphasized by Kohn (51), while retaining the accuracy of the original XYGJ OS (described below).

Thus our proposed functional form (XYGJ OS) is

$$E_{xc}^{\text{XYGJ OS}}[\rho] = e_x E_x^{\text{HF}} + (1 - e_x) E_x^{\text{S}} + (e_{\text{VWN}} E_c^{\text{VWN}} + e_{\text{LYP}} E_c^{\text{LYP}}) + e_{\text{PT2}} E_{c,\text{OS}}^{\text{PT2}}. \quad [\text{S12}]$$

In Eq. S12 we normalize the HF exchange and Slater exchange, while eliminating the  $\Delta E_x^{\text{GGA}}$  contribution. The superscript “PT2” indicates that only the MP2 like perturbation part in Eq. S7 is evaluated as also done in the B2PLYP (19) and other DHDFs (17, 20, 21). The correlation part consists of  $E_c^{\text{VWN}}$ ,  $E_c^{\text{LYP}}$ , and  $E_{c,\text{OS}}^{\text{PT2}}$ , where the first term includes both the SS and OS effects while the second and third terms include only OS components. Our concept is that the combination of VWN, LYP, and PT2 OS yields a balanced description of both local and nonlocal spin dependent correlation terms. To determine the optimal four parameters in Eq. S12, we use the experimental HOF data for the G3/99 set of 223 molecules (24–26) as the training set, leading to  $\{e_x, e_{\text{VWN}}, e_{\text{LYP}}, e_{\text{PT2}}\} = \{0.7731, 0.2309, 0.2754, 0.4364\}$ .

We would like to emphasize that we use fully optimized B3LYP orbitals to generate the density and to calculate each term in Eq. S12 (17, 44, 45, 46). Other DHDFs have either used HF orbitals for PT2 evaluation (18), or the density and orbitals from a truncated functional with incomplete correlation (19–21, 47–49).

**Summary of local OS PT2 approximations.** In this section of SI, we summarize the approximations associated with the local OS PT2 ansatz, and a brief introduction of how the locality is exploited in the present algorithm. That is, we here summarize ref. 31 for completeness.

In order to be able to use locality of electron correlation, one has to transform the canonical orbital based PT2 expression to the local orbital based expression. To this end, we eliminate the energy denominator via the Laplace transform  $1/x = \int_0^\infty dt e^{-xt}$  (56):

$$E_{\text{OS PT2}} = - \sum_{ia}^\alpha \sum_{jb}^\beta \frac{(ia|jb)^2}{\varepsilon_a + \varepsilon_b - \varepsilon_i - \varepsilon_j} = - \int_0^\infty dt \sum_{ia}^\alpha \sum_{jb}^\beta e^{-(\varepsilon_a + \varepsilon_b - \varepsilon_i - \varepsilon_j)t} (ia|jb)^2, \quad [\text{S13}]$$

where  $\varepsilon_i, \varepsilon_j, \varepsilon_a, \varepsilon_b$  are the orbital energies of the occupied levels  $i, j$  and the virtual levels  $a, b$ . The two electron MO repulsion integrals are given by:

$$\langle ij|ab \rangle = (ia|jb) = \int d\mathbf{r}_1 \int d\mathbf{r}_2 \phi_i(\mathbf{r}_1) \phi_a(\mathbf{r}_1) \frac{1}{|\mathbf{r}_1 - \mathbf{r}_2|} \phi_j(\mathbf{r}_2) \phi_b(\mathbf{r}_2). \quad [\text{S14}]$$

Numerical integration over  $t$  is performed by introducing a discrete quadrature (over  $n$  points, which is typically 6–8):

$$E_{\text{OS PT2}} = - \sum_q^n w_q \sum_{ia}^\alpha \sum_{jb}^\beta e^{-(\varepsilon_a + \varepsilon_b - \varepsilon_i - \varepsilon_j)t_q} (ia|jb)^2 = - \sum_q^n w_q \sum_{ia}^\alpha \sum_{jb}^\beta (\tilde{i}\tilde{a}|\tilde{j}\tilde{b})_q^2. \quad [\text{S15}]$$

$t$  dependent Laplace transformed orbitals  $\tilde{\phi}_i$  and  $\tilde{\phi}_a$  are given in terms of canonical orbitals that are exponentially damped:

$$\tilde{\phi}_i = \phi_i e^{\varepsilon_i t_q/2} \quad [\text{S16}]$$

$$\tilde{\phi}_a = \phi_a e^{-\varepsilon_a t_q/2}. \quad [\text{S17}]$$

In Eqs. S16, S17 and below, we use a notation for simplicity that  $\tilde{\phi}_i$  implies the transformed orbital at the quadrature point  $q$ . We next introduce an auxiliary basis  $\{\Phi_Q\}$  expansion for the product density (Eq. S18) to reduce the number of expensive four center two electron integrals into much more affordable two- and three center integrals.

$$\rho = |\varphi_i \varphi_a\rangle \approx \rho_{\text{fitted}} = \sum_Q^M C_Q^{ia} |\Phi_Q\rangle. \quad [\text{S18}]$$

This approximation is also known as Resolution of Identity (RI) or density fitting technique (53, 54). The auxiliary basis expansion coefficients,  $C$ , are determined by minimizing the self interaction of the difference between the fitted distribution and the actual distribution,  $\rho_{\text{diff}} = \rho_{\text{fitted}} - \rho_{\text{actual}}$ , defined as,

$$(\rho_{\text{diff}}|\rho_{\text{diff}}) = \int d\mathbf{r}_1 \int d\mathbf{r}_2 \rho_{\text{diff}}(\mathbf{r}_1) g(\mathbf{r}_1, \mathbf{r}_2) \rho_{\text{diff}}(\mathbf{r}_2), \quad [\text{S19}]$$

where  $g(\mathbf{r}_1, \mathbf{r}_2) = 1/|\mathbf{r}_1 - \mathbf{r}_2|$ . Differentiation of Eq. S19 with respect to  $C$  and setting it to zero leads to the following solution for  $C$ , which involves only the two index two electron and three index two electron integrals:

$$C_Q^{ia} = \sum_P (\tilde{i}\tilde{a}|P)(P|Q)^{-1}. \quad [\text{S20}]$$

Inserting Eqs. S18 and S20 into Eq. S14 results in the following integral approximation:

$$(\tilde{i}\tilde{a}|\tilde{j}\tilde{b}) \approx \sum_Q B_Q^{ia} B_Q^{jb}, \quad [\text{S21}]$$

where  $B$  is the matrix defined as:

$$B_Q^{ia} = \sum_P (\tilde{i}\tilde{a}|P)(P|Q)^{-1/2}. \quad [\text{S22}]$$

Substituting Eq. S21 into Eq. S15 finally leads to the following working expression for the OS PT2 correlation energy:

$$E_{\text{OS PT2}} = - \sum_q^n w_q \sum_{PQ} X_{PQ} \bar{X}_{PQ}. \quad [\text{S23}]$$

$X_{PQ}$  and  $\bar{X}_{PQ}$  are defined as:

$$X_{PQ} = \sum_{ia}^\alpha B_P^{ia} B_Q^{ia} \quad [\text{S24}]$$

$$\bar{X}_{PQ} = \sum_{jb}^\beta B_P^{jb} B_Q^{jb}. \quad [\text{S25}]$$

Formation of  $X$  from the  $B$  matrices, Eqs. S24 and S25, is the most expensive fourth order step in OS PT2.

While Eq. S15 is specific to the canonical orbital basis, expressions in a generalized orthogonal basis can be given as follows:

$$E_{\text{OS PT2}} = - \sum_q w_q \sum_{IA}^{\alpha} \sum_{JB}^{\beta} (\tilde{I}\tilde{A}|\tilde{J}\tilde{B})_q^2 \quad [\text{S26}]$$

$$\tilde{\phi}_I = \sum_K \phi_K (\phi_K | e^{\hat{t}_q/2} | \phi_I) = \sum_K \phi_K W_{KI} \quad [\text{S27}]$$

$$\tilde{\phi}_A = \sum_C \phi_C (\phi_C | e^{\hat{t}_q/2} | \phi_A) = \sum_C \phi_C W_{CA}, \quad [\text{S28}]$$

where indices  $I, J, K, \dots$  and  $A, B, C, \dots$  refer to localized functions that span occupied and virtual spaces. In Eqs. S27 and S28, we again assume that  $\tilde{\phi}_I$  implies the transformed orbital at the quadrature point  $q$ . We chose to use orthogonal Boys functions for the localized occupied orbitals, and the generalized orthogonal projected atomic orbitals (AO)'s for the localized virtual orbitals, defined as  $|A\rangle = \hat{Q}(s^{-1/2})|\mu\rangle$ , where  $\hat{Q}$  is the virtual projection operator, and  $\mu, \nu, \dots$  are the AO indices. We could have used Boys virtual orbitals instead of the projected AOs since the projected AOs partly destroy the locality of AOs by applying  $s^{-1/2}$ . But Boys localization using the Jacobi sweeps becomes computationally very demanding due to poor convergence for large systems. Therefore we used the projected AOs for the localization of virtual orbitals.

We next introduce the auxiliary basis expansion, as before, for the product distribution  $\tilde{\phi}_I \tilde{\phi}_A$ , and obtain the same solution for  $C$ , except that here we choose to employ the short range two electron operator  $g(\mathbf{r}_1, \mathbf{r}_2) = \text{erfc}(\omega|\mathbf{r}_1 - \mathbf{r}_2|)/|\mathbf{r}_1 - \mathbf{r}_2|$ , which is denoted with a subscript  $\omega$ , to remove the long range artifact of Coulomb metric (55).

$$C_Q^{IA} = \sum_P (\tilde{I}\tilde{A}|P)_\omega (P|Q)_\omega^{-1}. \quad [\text{S29}]$$

Finally, we rewrite Eq. S14 as the following working expression for the local OS PT2 algorithm:

$$E_{\text{OS PT2}} = - \sum_q w_q \sum_{PQRS} Y_{PR} (P|Q) \tilde{Y}_{QS} (R|S) \quad [\text{S30}]$$

$$Y_{PR} = \sum_{IA}^{\alpha} C_P^{IA} C_R^{IA} \quad [\text{S31}]$$

$$\tilde{Y}_{QS} = \sum_{JB}^{\beta} C_Q^{JB} C_S^{JB}. \quad [\text{S32}]$$

To exploit the locality and sparsity of the various matrices, we use a scheme called “natural blocking,” where the entire rows or columns of large matrices can be removed for processing due to the physical nature (structure) of given matrices.

Eq. S31 is the most time consuming step in a straightforward 4th order scaling implementation of OS PT2 method (like

Eqs. S24 and S25). But because the occupied and virtual functions ( $I, A$ ) are localized and the auxiliary expansion functions  $Q$  are also local, the fitting coefficients  $C_Q^{IA}$  (where the quadrature point  $q$  is implied as in Eq. S27 and S28) must also be local. In other words, for a given occupied orbital  $I$ , only those virtual and auxiliary functions (matrix elements) that are local to  $I$  will be nonzero, and so  $Y_{PQ} = \sum_B C_P^{IB} C_Q^{IB} + (P_{\text{sig}} B_{\text{sig}})_I (B_{\text{sig}} Q_{\text{sig}})_I$ , where  $P_{\text{sig}}, B_{\text{sig}}, Q_{\text{sig}}$  mean that  $P, B$ , and  $Q$  are local to  $I$ , can be evaluated with a linear scaling effort. In a natural blocking scheme, the  $(P, B)$  batches of the three index C “matrix” are examined and the entire rows and columns are removed if they are not local to  $I$ . Furthermore,  $C_Q^{IA}$  is arranged optimally for this operation, which is performed as an efficient dense matrix multiply over the significant virtual ( $B_{\text{sig}}$ ) and auxiliary ( $P_{\text{sig}}$ ) indices, using the natural blocking scheme. In deleting the rows and columns, we have used a numerical cutoff of  $5 \times 10^{-6}$  and the error associated with it is insignificant as shown below.

In another step, the AO to occupied MO transformation  $(I\nu|P)_\omega = \sum_\mu C_{\mu I}(\mu\nu|P)_\omega$  is  $O(M^4)$  work. For a large enough system, it asymptotically approaches  $O(M^3)$  because the magnitude of the  $\mu\nu$  function product decays as a Gaussian with the inter function distance. Because the integral operator is short ranged, as denoted by a subscript  $\omega$ , only those integrals that involve basis functions ( $\mu, \nu$ , and  $P$ ) that are close each other in real space will have nonzero values. A significant number of arithmetic operations can be saved by using this integral sparsity, namely by inserting an IF statement in which the first MO transformation is skipped if the integral value is zero against some numerical threshold. We have used  $10^{-6}$  as an integral threshold criterion, which is sufficiently tight that it adds no additional error numerically as shown below. This utilization of sparsity makes the cost of occupied index AO to MO transformation formally  $O(M^2)$ , instead of  $O(M^3)$ .

Other steps involved in the transformations and evaluations of various quantities that lead to Eqs. S31 and S32 have also been accelerated by using the similar blocking scheme and integral screening (see ref. 35 for more details). The resulting algorithm is formally cubic scaling (localization, local transformation, and inspection of the matrices), but due to a relatively small prefactor of the latter cubic steps it shows a quadratic scaling for favorable cases before these cubic steps become dominant.

As seen in Fig. S3, linear alkane chains show a quadratic scaling and a significant speedup as compared to the calculation with out using local algorithm. On the other hand, the fully three dimensional (3D) dense systems like the diamond do not show a significant speedup up to C100 due to the small length scale of this system even with 100 carbon atoms,  $\approx 10 \text{ \AA}$ . In contrast, the length scale of linear alkane with 100 carbon atoms is about  $\approx 125 \text{ \AA}$ , thus showing a substantial speedup. This relatively modest speedup means that, for fully 3D structures like the diamond structure, we have simply not yet reached the quadratic or cubic regime where sparsity can make a significant difference. There will be a significant speedup using the local algorithm even for dense 3D systems, however, if one considers large enough systems. The memory and disk requirement for the local PT2 calculation are also quadratically scaling, moderate to be applicable for large systems.

1. Furche F, Perdew JP (2006) The performance of semilocal and hybrid density functionals in 3d transition-metal chemistry. *J Chem Phys* 124:1–27.
2. Slater JC (1974) *Quantum Theory of Molecules and Solids*, v.4.(McGraw-Hill, New York).
3. Vosko SH, Wilk L, Nusair M (1980) Accurate spin-dependent electron liquid correlation energies for local spin-density calculation—A critical analysis. *Can J Phys* 58:1200–1211.
4. Becke AD (1988) Density-functional exchange-energy approximation with correct asymptotic behavior. *Phys Rev A* 38:3098–3100.

5. Lee CT, Yang WT, Parr RG (1988) Development of the collesalvetti correlation-energy formula into a functional of the electron-density. *Phys Rev B* 37:785–789.
6. Perdew JP (1991) *Electronic Structure of Solids '91*, edited by Ziesche P, Eschrig P.11. (Akademie Verlag, Berlin).
7. Perdew JP, Wang Y (1992) Accurate and simple analytic representation of the electron-gas correlation energy. *Phys Rev B* 45:13244–13249.
8. Perdew J, Burke K, Ernzerhof M (1996) Generalized gradient approximation made simple. *Phys Rev Lett* 77:3865–3868.

9. Zhao Y, Truhlar DG (2006) A new local density functional for main-group thermochemistry, transition metal bonding, thermochemical kinetics, and noncovalent interactions. *J Chem Phys* 125:1–18.
10. Tao J, Perdew J, Staroverov V, Scuseria G (2003) Climbing the density functional ladder: Nonempirical meta-generalized gradient approximation designed for molecules and solids. *Phys Rev Lett* 91:1–4.
11. Becke AD (1993) Density-functional thermochemistry 3: The role of exact exchange. *J Chem Phys* 98:5648–5652.
12. Stephens PJ, Devlin FJ, Chabalowski CF, Frisch MJ (1994) Ab-initio calculation of vibrational absorption and circular-dichroism spectra using density-functional force-fields. *J Phys Chem* 98:11623–11627.
13. Becke AD (1992) Density-functional thermochemistry 2: The effect of the exchange-only gradient correction. *J Chem Phys* 96:2155–2160.
14. Xu X, Goddard WA (2004) The X3LYP extended density functional for accurate descriptions of nonbond interactions, spin states, and thermochemical properties. *Proc Natl Acad Sci USA* 101:2673–2677.
15. Adamo C, Barone V (1998) Exchange functionals with improved long-range behavior and adiabatic connection methods without adjustable parameters: The mPW and mPW1PW models. *J Chem Phys* 108:664–675.
16. Zhao Y, Truhlar DG (2008) The M06 suite of density functionals for main group thermochemistry, thermochemical kinetics, noncovalent interactions, excited states, and transition elements: two new functionals and systematic testing of four M06-class functionals and 12 other functionals. *Theor Chem Acc* 120:215–241.
17. Zhang Y, Xu X, Goddard WA, III (2009) Doubly hybrid density functional for accurate description of nonbond interactions, thermochemistry, and thermochemical kinetics. *Proc Natl Acad Sci USA* 106:4963–4968.
18. Zhao Y, Lynch BJ, Truhlar DG (2004) Doubly hybrid meta DFT: New multicoefficient correlation and density functional methods for thermochemistry and thermochemical kinetics. *J Phys Chem A* 108:4786–4791.
19. Grimme S (2006) Semiempirical hybrid density functional with perturbative second-order correlation. *J Chem Phys* 124:1–16.
20. Karton A, Tarnopolsky A, Lamère J-F, Schatz GC, Martin JML (2008) Highly accurate first-principles benchmark datasets for the parametrization and validation of density functional and other approximate methods. Derivation of a robust, generally applicable, double-hybrid functional for thermochemistry and thermochemical kinetics. *J Phys Chem A* 112:12868–12886.
21. Chai JD, Head-Gordon M (2009) Long-range corrected double-hybrid density functionals. *J Chem Phys* 131:1–13.
22. Schwabe T, Grimme S (2007) Double-hybrid density functionals with long-range dispersion corrections: higher accuracy and extended applicability. *Phys Chem Chem Phys* 9:3397–3406.
23. Grimme S (2006) Semiempirical hybrid density functional with perturbative second-order correlation. *J Chem Phys* 124:1–16.
24. Curtiss LA, Redfern PC, Raghavachari K, Pople JA (2001) Gaussian-3X (G3X) theory: Use of improved geometries, zero-point energies, and Hartree-Fock basis sets. *J Chem Phys* 114:108–117.
25. Curtiss LA, Raghavachari K, Redfern PC, Rassolov V, Pople JA (1998) Gaussian-3 (G3) theory for molecules containing first and second-row atoms. *J Chem Phys* 109:7764–7776.
26. Curtiss LA, Raghavachari K, Redfern PC, Pople JA (2000) Assessment of Gaussian-3 and density functional theories for a larger experimental test set. *J Chem Phys* 112:7374–7383.
27. Wu JM, Xu X (2007) The X1 method for accurate and efficient prediction of heats of formation. *J Chem Phys* 127:214105–214113.
28. Zhao Y, González-García N, Truhlar DG (2005) Benchmark database of barrier heights for heavy-atom transfer, nucleophilic substitution, association, and unimolecular reactions and its use to test theoretical methods. *J Phys Chem A* 109:2012–2018.
29. Zhao Y, Truhlar DG (2005) Design of density functionals that are broadly accurate for thermochemistry, thermochemical kinetics, and nonbonded interactions. *J Phys Chem A* 109:5656–5667.
30. Grimme S (2003) Improved second-order Møller-Plesset perturbation theory by separate scaling of parallel- and antiparallel-spin pair correlation energies. *J Chem Phys* 118:9095–9102.
31. Jung YS, Lochan RC, Dutoi AD, Head-Gordon M (2004) Scaled opposite-spin second order Møller-Plesset correlation energy: an economical electronic structure method. *J Chem Phys* 121:9793–9802.
32. Zhang LL, Lu YP, Lee S-Y, Zhang DH, (2007) A transition state wave packet study of the H + CH<sub>4</sub> reaction. *J Chem Phys* 127:1–7.
33. Takatani T, Sherrill CD (2007) Performance of spin-component-scaled Møller-Plesset theory (SCS-MP2) for potential energy curves of noncovalent interactions. *Phys Chem Chem Phys* 9:6106–6114.
34. Jung YS, Shao YH, Head-Gordon M (2007) Fast evaluation of scaled opposite-spin second-order Møller-Plesset correlation energies using auxiliary basis expansions and exploiting sparsity. *J Comput Chem* 28:1953–1964.
35. Jung YS, Shao YH, Head-Gordon M (2007) Fast evaluation of scaled opposite-spin second-order Møller-Plesset correlation energies using auxiliary basis expansions and exploiting sparsity. *J Comput Chem* 28:1953–1964.
36. Shao Y, et al. (2006) Advances in methods and algorithms in a modern quantum chemistry program package. *Phys Chem Chem Phys* 8:3172–3191.
37. Hohenberg P, Kohn W (1964) Inhomogeneous electron gas. *Phys Rev B* 136:864–887.
38. Levy M (1979) Universal variational functionals of electron densities, 1st-order density matrices, and natural spin-orbitals and solution of the V-representability problem. *Proc Natl Acad Sci USA* 76:6062–6065.
39. Kohn W, Sham LJ (1965) Self-consistent equations including exchange and correlation effects. *Phys Rev* 140:1133–1138.
40. Mori-Sánchez P, Cohen AJ, Yang WT (2006) Many-electron self-interaction error in approximate density functionals. *J Chem Phys* 125:1–4.
41. Gunnarsson O, Lundqvist B (1976) Exchange and correlation in atoms, molecules, and solids by the spin-density-functional formalism. *Phys Rev B* 13:4274–4298.
42. Levy M, Perdew JP (1985) Hellmann-Feynman, virial and scaling requisites for the exact universal density functional—shape of the correlation potential and diamagnetic susceptibility for atoms. *Phys Rev A* 32:2010–2021.
43. Görling A, Levy M (1993) Correlation-energy functional and its high-density limit obtained from a coupling-constant perturbation expansion. *Phys Rev B* 47:13105–13113.
44. Zhang IY, Luo Y, Xu X (2010) XYG3s: Speedup of the XYG3 fifth-rung density functional with scaling-all-correlation method. *J Chem Phys* 132:1–11.
45. Zhang IY, Wu JM, Luo Y, Xu X (2010) Trends in R-X bond dissociation energies (R = Me, Et, i-Pr, t-Bu, X = H, Me, Cl, OH). *J Chem Theory Comput* 6:1462–1469.
46. Zhang IY, Wu JM, Xu X (2010) Extending the reliability and applicability of B3LYP. *Chem Comm* 46:3057–3070.
47. Sancho-García JC, Pérez-Jiménez AJ (2009) Assessment of double-hybrid energy functionals for pi-conjugated systems. *J Chem Phys* 131:1–11.
48. Graham DC, Menon AS, Goerigk L, Grimme S, Radom L (2009) Optimization and basis-set dependence of a restricted-open-shell form of B2-PLYP double-hybrid density functional theory. *J Chem Phys* 131:9861–9873.
49. Benighaus T, DiStasio A, Lochan R, Chai JD, Head-Gordon M (2008) Semiempirical double-hybrid density functional with improved description of long-range correlation. *J Phys Chem A* 112:2702–2712.
50. Becke AD (1993) A new mixing of Hartree-Fock and local density-functional theories. *J Chem Phys* 98:1372–1377.
51. Kohn W (1996) Density functional and density matrix method scaling linearly with the number of atoms. *Phys Rev Lett* 76:3168–3171.
52. Almlöf J (1991) Elimination of energy denominators in Møller-Plesset perturbation theory by a Laplace transform approach. *Chem Phys Lett* 181:319–320.
53. Feyereisen M, Fitzgerald G, Komornicki A (1993) Use of approximate integrals in abinitio theory—An application in MP2 energy calculations. *Chem Phys Lett* 208:359–363.
54. Weigend F, Haser M, Patzelt H, Ahlrichs R (1998) RI-MP2: optimized auxiliary basis sets and demonstration of efficiency. *Chem Phys Lett* 294:143–152.
55. Jung Y, Sodt A, Gill PMW, Head-Gordon M (2005) Auxiliary basis expansions for large-scale electronic structure calculations. *Proc Natl Acad Sci USA* 102:6692–6697.
56. Goerigk L, Grimme S (2010) A general database for main group thermochemistry, kinetics, and noncovalent interactions—Assessment of common and reparameterized (meta-)GGA density functionals. *J Chem Theor Comp* 6:107–126.
57. Goerigk L, Grimme S (2011) A thorough benchmark of density functional methods for general main group thermochemistry, kinetics, and noncovalent interactions. *Phys Chem Chem Phys* 13:6670–6688.







**Table S1. Mean absolute deviations (MADs, in kcal/mol) for various benchmark sets with the G3Large basis set. BSSE correction is not included unless otherwise stated**

	Methods	HOF (223)	IP (38)	EA (25)	PA (8)	BDE (92)	NHTBH (38)	HTBH (38)	NCIE (31)	All (493)
1st rung	SVWN (SPL)	130.88	15.14	17.30	5.68	18.14	12.53	17.95	3.29	67.28
2nd	BLYP	10.16	6.02	2.47	1.75	7.00	8.29	7.68	1.49	7.84
Rung	PW91	22.04	5.19	3.19	1.53	3.75	8.95	9.76	1.31	12.78
	PBE	20.71	5.13	2.40	1.56	3.91	8.57	9.48	1.17	12.10
3rd	M06 L	5.20	5.31	3.56	1.60	4.17	3.81	4.33	0.59	4.41
Rung	TPSS	5.01	5.36	2.41	1.66	5.88	9.04	8.26	1.14	5.33
4th	B3LYP	6.08	3.74	2.45	1.40	5.51	4.84	4.26	0.98	4.98
Rung	B3LYP D	3.58	3.77	2.46	1.09	4.16	5.22	5.21	0.65	3.67
	B3LYP D3	4.15	3.77	2.47	1.18	4.29	5.17	4.97	0.64	3.93
	X3LYP	5.04	3.69	2.11	1.62	5.09	4.70	4.52	0.84	4.41
	PBE0	5.64	3.84	2.97	1.25	3.67	3.56	4.38	0.71	4.36
	M06 2X	2.26	2.72	2.37	1.94	1.40	1.26	1.25	0.28	1.86
	M06	3.37	3.63	2.04	1.78	1.95	2.31	2.16	0.43	2.67
5th	XYG3	3.44	1.30	1.98	1.65	1.86	1.31	0.81	0.32	2.31
	XYG3*	1.81	1.31	1.84	1.61	1.56	1.29	0.75	0.32	1.51
Rung	XYGJ OS	<b>1.65</b>	<b>1.23</b>	<b>1.97</b>	<b>1.68</b>	<b>0.71</b>	<b>1.18</b>	<b>0.87</b>	<b>0.35</b>	<b>1.28</b>
	MC3BB	3.28	2.78	4.01	1.03	2.43	1.44	0.80	0.58	2.58
	B2PLYP	7.59	2.48	2.15	1.52	3.30	2.23	1.73	0.55	4.71
	B2PLYP <sup>†</sup>	2.74 <sup>†</sup>	2.48	2.15	1.52	2.95 <sup>†</sup>	2.23	1.73	0.55	2.45
	B2PLYP D	5.89	2.48	2.15	1.34	2.60	2.47	2.11	0.45	3.85
	B2PLYP D <sup>†</sup>	1.67 <sup>†</sup>	2.48	2.15	1.34	2.27 <sup>†</sup>	2.47	2.11	0.45	1.88
	B2GP LYP	7.95	2.24	2.72	1.44	2.72	1.36	0.70	0.40	4.62
	ωB97X 2(LP)	5.34	1.62	1.53	1.52	1.82	1.95	0.71	0.73	3.23
	ωB97X 2(LP) <sup>‡</sup>	1.52	1.73	1.56	1.09	1.62	1.67	0.74	0.47 <sup>§</sup>	1.44
Ab initio	HF	213.42	23.19	26.46	3.09	32.70	9.08	13.51	2.37	107.71
	MP2	10.63	3.49	3.59	2.13	7.73	5.42	3.91	0.60	7.49
	SCS MP2	11.64	4.02	4.94	1.02	6.23	6.53	5.22	0.32	7.93
	SOS MP2	15.07	4.52	5.82	0.89	6.01	7.09	6.09	0.46	9.64
	G2	1.89	0.97	1.31	1.34	1.80	0.97	1.24	0.57	1.56
	G3	1.06	1.27	1.13	1.06	1.08	0.97	1.24	0.57	1.06

\*Taken from ref. 17 with 6-311+G(3df,2p).

<sup>†</sup>HOF are taken from ref. 22 with very large basis set of CQZV3P. BDEs are calculated using the corresponding HOF.

<sup>‡</sup>Taken from ref. 21 or calculated with 6-311++G(3df,3pd).

<sup>§</sup>BSSE corrections are included for the NCIE set.

**Table S2. Mean absolute deviation for RBH of Truhlar's NHTBH38 and HTBH38 sets (basis sets: 6-311+G(3df,2p))**

RBH	UM10	NS16	HAT12	HT38	NHT38	Total
B3LYP	2.02	3.38	8.50	4.31	4.64	4.47
B3LYP D	2.50	4.03	8.96	5.06	5.18	5.12
B3LYP D3	2.37	4.01	8.93	4.83	5.13	4.98

Here HT38 refers to the forward and reverse barrier heights for 19 hydrogen transfer reactions; HAT12 refers to the forward and reverse barrier heights for six heavy atom transfer reactions, NS16 refers to the forward and reverse barrier heights for eight nucleophilic substitution reactions and UM10 refers to the forward and reverse barrier heights for five association and unimolecular reactions).

**Table S3. Mean absolute deviation for Truhlar's NCIE31 set of nonbonded interactions (basis sets: 6-311+G(3df,2p))**

RBH	HB6	CT7	DI6	WI7	PP55	Total(31)	
B3LYP	0.63	0.76	0.61	0.27	2.93	0.95	
	BSSE corrected	0.55	0.76	0.93	0.38	3.25	1.07
B3LYP D	0.86	1.49	0.60	0.14	0.34	0.71	
	BSSE corrected	1.07	1.40	0.33	0.04	0.46	0.67
B3LYP D3	0.70	1.60	0.78	0.11	0.21	0.70	
	BSSE corrected	0.93	1.48	0.46	0.01	0.29	0.65

NCIE31 consists of six hydrogen bond (HB) complexes, seven charge transfer (CT) complexes, six dipole interaction (DI) complexes, seven weak interaction (WI) complexes, and five  $\pi$ - $\pi$  stacking (PPS) complexes. The WI and PPS are dominated by London dispersion)